PARALLEL COMPUTATION OF TWO-DIMENSIONAL LINEARIZED EULER EQUATIONS

Jônatas Ferreira Lacerda, jonatasflacerda@hotmail.com
Leandro Franco de Souza, lefraso@icmc.usp.br
Josuel Kruppa Rogenski, josuelkr@gmail.com
Departamento de Matemática Aplicada e Estatística – ICMC – USP Av. Trabalhador São Carlense, 400, CEP:13560-970 São Carlos - SP

Abstract. *Perform numerical analysis of sound generation and propagation with accuracy and with lower computational time are some of the main challenges for Computational Aeroacoustics (CAA), which had experienced some major improvements in the last decade. In the present work it was performed numerical study of two-dimensional propagation of waves by solving LEE equations applied to a Gaussian pulse in pressure and density in an undisturbed mean flow with different Mach numbers. A 4^{th}-order 4-steps Runge-Kutta scheme was adopted for time integration. The spatial derivatives were calculated by a 4^{th}-order DRP and a 6^{th}-order compact finite difference schemes. Additionally, the problem was parallelized adopting MPI using 1-D and 2-D domain decompositions. A speed-up and efficiency analysis showed that the computation time is reduced using this technique, being more effective for the compact finite difference scheme. However, there was a decrease in efficiency probably due time spent in communication and synchronization.*

Keywords: *Computational Aeroacoustics, Linearized Euler Equations, Parallel Computation, Domain Decomposition, MPI.*

1. INTRODUCTION

The early studies of sound generated aerodynamically were based in the acoustic analogy given by Lighthill (1952) and Lighthill (1954), by which the real problem involving a highly disturbed flow is restated as a problem of linear acoustics in a medium at rest with equivalent acoustic sources. Further developments of Lighthill's work were made by Ffowcs Williams and Hawkings (1969) to include the presence of moving surfaces, for application to the noise from aerodynamic rotors, among others.

These analogies have been used together with unsteady data provided by Computational Fluid Dynamic (CFD) calculations to predict sound generated by complex flow (Wang *et al.*, 2006; Y. Kalighi and Moin, 2008). Such procedure is commonly known as hybrid simulation because the flow field is simulated separately from the acoustic field, with the computation of the sound being some kind of post-processing of flow analysis. Thus, Wang *et al.* (2006) classify acoustic analogies as modelling which should be applied with caution.

A different approach to predict sound generation and its propagation in a mean flow is to compute simultaneously the flow and acoustic fields. Standard CFD schemes are generally not adequate due some particularities related to aeroacoustics problems: time-dependency, wide bandwidth frequency range, different scales (acoustic waves amplitudes are very small compared to mean flow amplitudes), propagation to long distance from the source and slowly decay of disturbances (Tam, 2006). These aspects impose some constraints over an aeroacoustics solver as: have extremely low numerical noise to does not affect the correct noise amplitude; have minimal numerical dispersion and dissipation to preserve the acoustic wave at long distances; and impose radiation boundary conditions to avoid reflection of outgoing sound waves from the computational domain (Tam, 2006).

All these approaches are part of recent research area commonly known as Computational Aeroacoustics (CAA), which had experienced some major improvements in the last decade. One aspect that contribute was the development of high resolution spatial discretization schemes obtaining less dispersive and less dissipative finite difference schemes with fewer points per wavelength (Lele, 1992; Tam and Webb, 1993). Another aspect was the development of better approaches to radiation boundary conditions (Hu, 1996, 2001; Tam *et al.*, 1998). However, even with these improvements, there is a increase demand in the numerical methods for aeroacoustics problems, because the mesh and accuracy requirements are higher. Therefore, the use of parallel computation is an excellent tool.

The main focus of the present paper is to perform a numerical study of two-dimensional propagation of waves by solving the two-dimensional linearized Euler equations (LEE). The numerical code initially used by Santana and Souza (2006a,b) was adopted here to perform the parallel numerical simulations. The spatial discretizations are performed using two different finite difference schemes: an explicit 4^{th}-order DRP scheme (Tam and Webb, 1993) and a 6^{th}-order compact finite difference scheme (Lele, 1992). A 4^{th}-order 4-steps Runge-Kutta scheme was adopted for time integration. Domain decomposition using Message Passage Interface (MPI) is used to perform parallel simulation. Speed-up and efficiency analysis are performed. The propagation of a Gaussian pulse in an undisturbed mean flow is simulated and compared with exact solution. The effects of the boundaries are not considered by stopping the simulation before the wave reached the domain boundaries. The paper is divided as folows: First, is presented the mathematical formulation used to study wave

propagations and then, the numerical method used to solve the problem. After that, is performed a code verification of the sequential and parallelized code. In the end are showed the results obtained for speed-up and efficiency analysis.

2. FORMULATION

To transport correctly aeroacoustic quantities, the Navier-Stokes (N-S) equations can be simplified. The Reynolds number based in the wave length is given by:

$$Re_\lambda \approx \frac{|\rho\frac{\partial u'}{\partial t}|}{|\mu\frac{\partial^2 u'}{\partial^2 t}|} \approx \frac{\lambda^2 f}{\nu}, \tag{1}$$

where λ is the wave length, f is the frequency and ν is the kinematic viscosity. For a typical problem of sound propagation in air, these parameters are $\nu = 1.4 \cdot 10^{-5}\ m^2/s$, $f = 20.0$ Hz up to 20.0 kHz (human audible range); $c_0 = 340\ m/s$ (sound velocity in air) and $\lambda = c_0/f = 0.34\ m$. These values leads to a typical Reynolds number of aeroacoustic problems of $Re_\lambda \approx 1 \cdot 10^7$ and $1 \cdot 10^5$, respectivelly, which is very high. Thus, the viscous terms of N-S equation are very small when compared with dynamic terms and can be neglected, leading to the Euler equations. Considering that the order of the terms related to acoustic propagation is very small when compared with the order of the terms of the fluid dynamic motion, it is possible to linearize the Euler equations over a reference base flow. Colonius *et al.* (1992) shows that this approach solves the problem with a smaller computational cost, without losing the quality of the numerical solution. The non-dimensional form of LEE can be obtained using: length scales $= \Delta x = \Delta y$, velocity scales $= c_0$, time scales $= \Delta x/c_0$, density scale $= \rho_0$, pressure scales $= \rho_0 c_0^2$, where Δx and Δy are the distance between two consecutive points in the *x* and *y* directions, respectively, and indices *0* corresponds to a reference state. Using these parameters, the non-dimensional LEE can be written as:

$$\frac{\partial \vec{u}}{\partial t} + \mathbf{A}\frac{\partial \vec{u}}{\partial x} + \mathbf{B}\frac{\partial \vec{u}}{\partial y} = \mathbf{H}^*, \tag{2}$$

where $\mathbf{H}^*$ is the non-dimensional source term related to the gradients of the mean flow, which are equal to zero when the mean flow is uniform, and

$$\vec{u} = \begin{pmatrix} \rho' \\ u' \\ v' \\ p' \end{pmatrix}, \qquad \mathbf{A} = \begin{pmatrix} M & 1 & 0 & 0 \\ 0 & M & 0 & 1 \\ 0 & 0 & M & 0 \\ 0 & 1 & 0 & M \end{pmatrix}, \qquad \mathbf{B} = \begin{pmatrix} 0 & 0 & 1 & 0 \\ 0 & 0 & 0 & 1 \\ 0 & 0 & 0 & 1 \\ 0 & 0 & 1 & 0 \end{pmatrix}, \tag{3}$$

are the respectively matrices, that are implemented in the numerical code. The terms $'$ represent small perturbations superimposed on the mean flow, which is used as a reference state.

2.1 Analytical solution of LEE for a pulse case

Tam and Webb (1993) presented the analytical solution of a two-dimensional Gaussian pulse on density and pressure fields, as initial condition, in a fluid at rest, based on Green function provided by Williams (1963) for the LEE on a Cartesian grid with constant mesh size. The initial conditions are defined as:

$$\begin{aligned} t &= 0, \\ p' &= \rho = \epsilon_1 e^{-\alpha_1 r^2}, \\ u' &= 0, \\ v' &= 0, \\ Ma &= 0.5 \end{aligned} \tag{4}$$

and the boundary conditions as:

$$\begin{cases} p' = 0 & \text{if } x = X_{max}, y = Y_{min} \text{ and } y = Y_{max}, \\ p' = \rho = v = 0 \text{ and } u = c_0 Ma & \text{at inflow and } x = X_{min}. \end{cases} \tag{5}$$

where Ma is the flow Mach number.

In Figs. 1(a) and 1(b) are presented the initial state and the time evolution of the pressure wave for the given boundary and initial conditions. As can be seen, there is a decay in the pulse amplitude, however, it is not due a diffusive behaviour, but due the increase in the area swept by the wave, since it conservs its total energy. The exact solution for velocity, pressure and density fields is given by:

$$u'(x,y,t) = \frac{\epsilon_1(x-Mt)}{2\alpha_1\eta}\int_0^\infty e^{\xi^2/4\alpha_1} sin(\xi t) J_1(\xi\eta)\xi d\xi, \tag{6}$$

$$v'(x,y,t) = \frac{\epsilon_1(y)}{2\alpha_1\eta}\int_0^\infty e^{\xi^2/4\alpha_1} sin(\xi t) J_1(\xi\eta)\xi d\xi, \tag{7}$$

$$p'(x,y,t) = \rho(x,y,t) = \frac{\epsilon_1}{2\alpha_1}\int_0^\infty e^{\xi^2/4\alpha_1} cos(\xi t) J_0(\xi\eta)\xi d\xi, \tag{8}$$

where $\eta = [(x-Mt)^2 + y^2]^{1/2}$, and J_0 and J_1 are the Bessel functions of zeroth and first order, respectively. The parameters used by Tam and Webb (1993) were pressure and density amplitude $\epsilon_1 = 0.01$, width at half height $b = 3.0$ and $\alpha_1 = ln(2)/b^2$, and is also used in the present work.

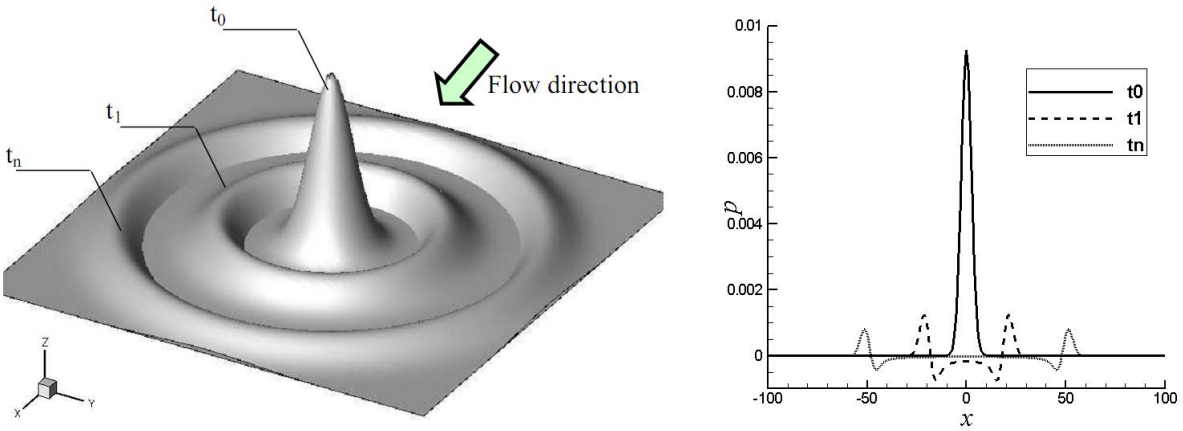

(a) (b)

Figure 1. (a) 3-d time evolution of a Gaussian pressure wave pulse pressure wave and (b) Gaussian pressure wave pulse pressure wave time evolution

3. NUMERICAL METHOD

The set of equations – Eq. (2), needs only the evaluation of first spatial derivatives. In the present work, these are calculated using two different finite difference schemes presented more detailed lately: an explicit 4^{th}-order DRP scheme and an implicit 6^{th}-order compact finite difference scheme. The time integration is performed using a 4^{th}-order 4-steps Runge-Kutta algorithm, which is commonly used in CAA. Considering a vector $\vec{u}$ that represents the solution values of spatial functions and $F(\vec{u})$ being the finite difference derivatives, the $n+1$ time step solution can be obtained by the following explicit low storage 4-*storage* scheme:

$$\begin{aligned} \vec{u}^0 &= \vec{u}^n \\ \vec{u}^i &= \vec{u}^n + \beta_i \Delta t F\left(\vec{u}^{i-1}\right) \qquad \text{for } i\text{=1,...,4} \\ \vec{u}^{n+1} &= \vec{u}^4 \end{aligned} \tag{9}$$

where are $\beta_1 = 1/4$, $\beta_2 = 1/3$, $\beta_3 = 1/2$ and $\beta_4 = 1$, respectively.

The numerical tests were performed using the sequential and the parallel codes. Initially it was performed a code verification of the sequential and parallel codes. The MPI was used to parallelize the code in two different ways: 1-D domain decomposition in x-direction (flow direction) and 2-D domain decomposition in both x- and y-directions. In the

case of 2-D domain decomposition the flow direction, which is the more interesting region, was more decomposed than transversal direction, as can be seen in Fig. 2 where are presented both domain decomposition strategies when used 8 processing elements. Afterward, speed-up and efficiency analysis were carried out to evaluate the parallel computation performance for both finite difference schemes.

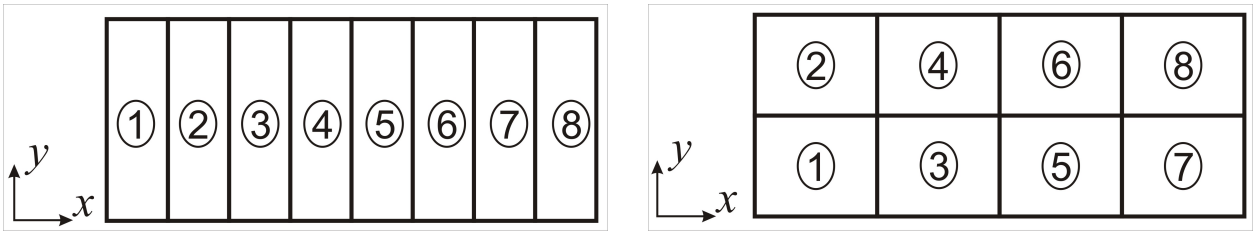

(a) (b)

Figure 2. (a) 1-D domain decomposition in x-axes and (b) 2-D domain decomposition in x- and y-axes

3.1 Finite difference schemes

Tam (2006) states that one of the basic needs of a CAA code is a scheme that can resolve high frequency short waves using fewer mesh points per wave length, which leaded to development of high resolution large stencil CAA schemes. According to the author, the Dispersion-Relation-Preserving (DRP) scheme of Tam and Webb (1993) and compact scheme reformulated by Lele (1992) are the most widely used schemes in CAA. Thus, in the present work a 4^{th}-order DRP scheme (Tam and Webb, 1993) and a 6^{th}-order compact finite difference scheme (Lele, 1992) are used to calculate the spatial derivatives.

The approximation of the first derivative, $f'(x_i)$, for DRP schemes can be obtained by solving Eq. (10), considering a mesh with uniform space h, indexing the nodes by *i* and the values at the nodes by $f(x_i)$.

$$f'(x_i) \cong \frac{1}{h} \sum_{j=-N}^{N} a_j f(x_i + jh) \tag{10}$$

where, for the DRP scheme used in the present work, N is equal three to obtain a five-point stencil, and the coefficients a_j are $a_1 = a_{-1} = 0.79926643$, $a_2 = a_{-2} = -0.18941314$ and $a_3 = a_{-3} = 0.02651995$, respectively.

The 6^{th}-order compact finite difference scheme (Lele, 1992) for the first derivatives is obtained by solving an algebraic system of equations formed by the generalised equation Eq. (11), applied to each nodal point:

$$a_{-1} f'_{i-1} + a_0 f'_i + a_1 f'_{i+1} = \frac{b_1}{12h}\left(f'_{i+1} - f'_{i-1}\right) + \frac{b_2}{12h}\left(f'_{i+2} - f'_{i-2}\right) \tag{11}$$

where $a_1 = a_{-1} = 1.0$, $a_0 = 3.0$, $b_1 = 28.0$ and $b_2 = 1.0$, respectively.

To analyse the finite difference schemes, their spectrum are analysed. Figure 3 shows the comparison between the effective wave number $\overline{k\Delta x}$ and the actual wave number $k\Delta x$ of each scheme used. As can be seen, the compact scheme (CP) curve remained closer to the exact solution (straight curve) than the obtained with the DRP scheme, for higher actual wave numbers. This means that this compact scheme is more accurate and can represent better higher wave numbers.

4. NUMERICAL VERIFICATION

The numerical verification of the sequential and parallel codes was performed using the Gaussian pulse case presented in section 2.1 As no special treatment at the boundaries was carried out to avoid reflection of the waves outgoing the computational domain, it was necessary to stop the simulation before the wave reached the domain boundaries. The residue error defined by Eq. (12) was used to compare the numerical solution p'_j with the exact solution p_j.

$$E_{RMS} = \frac{1}{N}\sqrt{\sum_{j=1}^{N}(p_j - p'_j)^2} \tag{12}$$

where N represents the total nodal points.

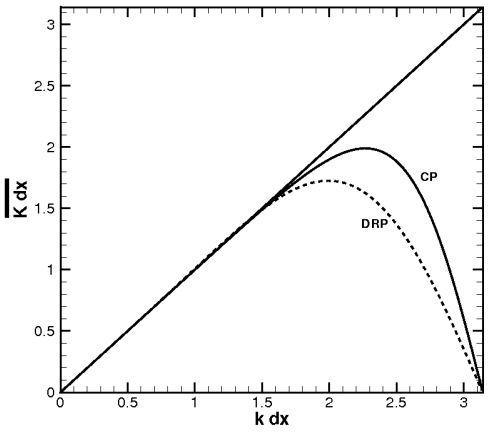

Figure 3. Effective and actual wave number comparison

4.1 Sequential Code

In a first step, it was performed the sequential code verification implemented with the DRP and compact finite difference schemes presented earlier. It was used a mesh with 558 x 558 points in each direction for Mach numbers equal 0; 0.25; 0.50 and 0.75. Figure 4 show a comparison of the pulse for $Ma = 0.50$ and $t = 100.0$. Figure 5(a) presents details at the pressure peaks where can be observed that the compact scheme shows better agreement with exact solution than for DRP scheme at the first pressure peak, but worst at the second peak. Figure 5(b) shows that DRP scheme present some oscilations near the non-disturbed region (high gradient region), mainly after the second peak. The E_{RMS} obtained for both schemes are presented in Tab. 1, showing that the compat scheme presented higher accuracy, except for $Ma = 0$. Furthermore, from the presented results the sequential code was satisfactorily verified.

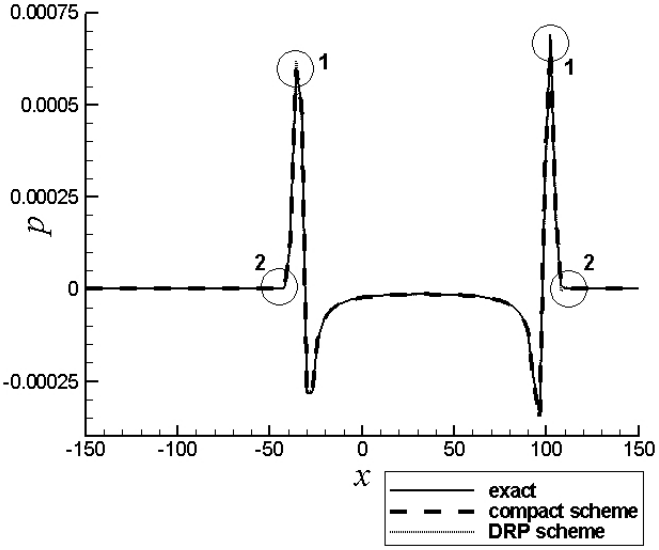

Figure 4. Pressure pulse comparison for $Ma = 0.50$ and $t = 100.0$.

Table 1. E_{RMS} for sequential code verification.

Mach Number	0.00	0.25	0.50	0.75
Compact scheme	$9.20 \cdot 10^{-9}$	$5.52 \cdot 10^{-9}$	$5.47 \cdot 10^{-9}$	$5.36 \cdot 10^{-9}$
DRP scheme	$6.52 \cdot 10^{-9}$	$5.96 \cdot 10^{-9}$	$5.77 \cdot 10^{-9}$	$5.54 \cdot 10^{-9}$

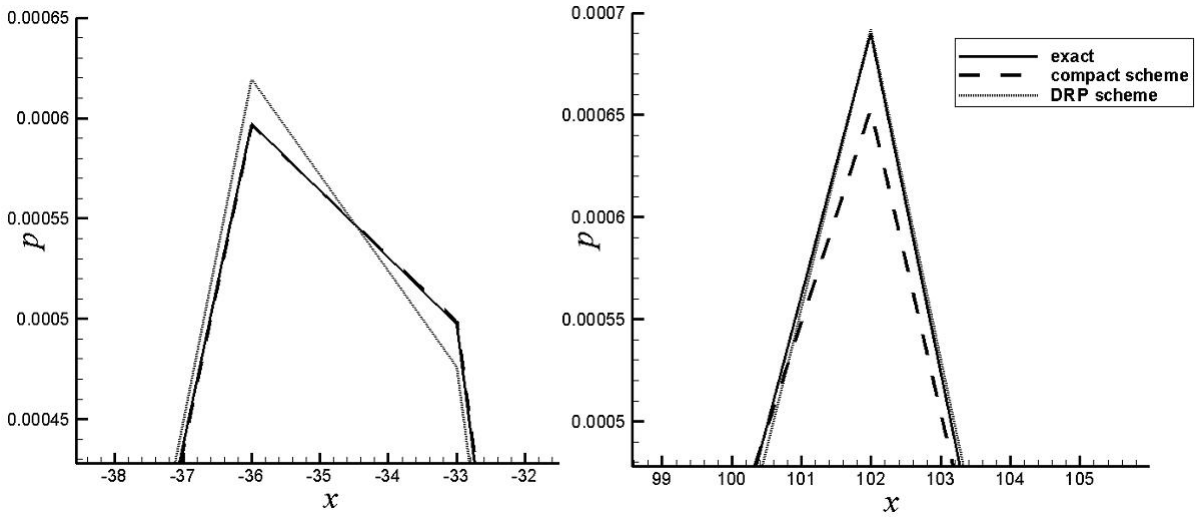

(a)

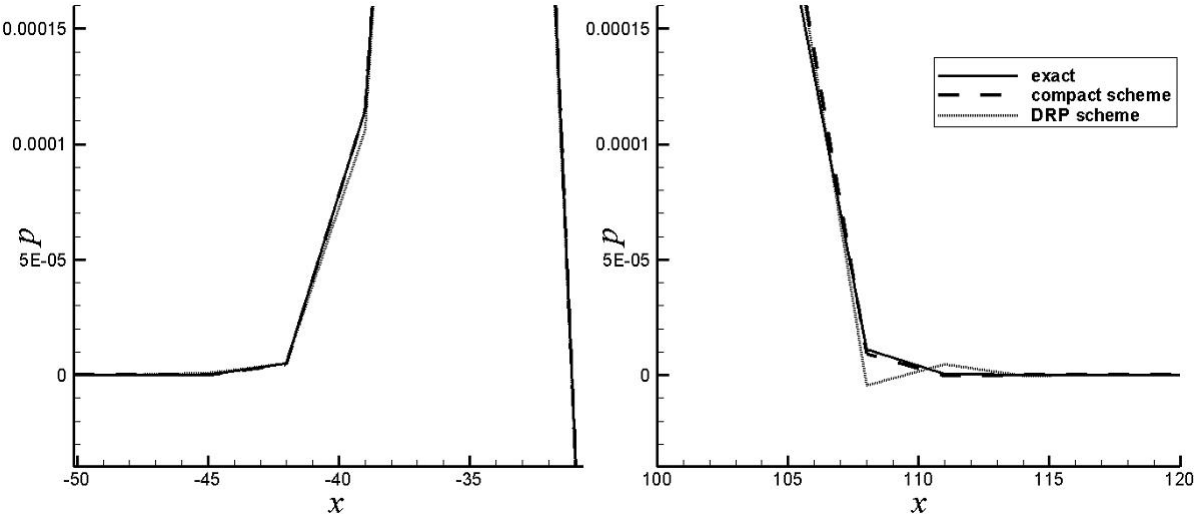

(b)

Figure 5. Comparison detail at (a) the peak and (b) near the non-disturbed region

4.2 Paralleled Code

In a second step, it was performed the parallel code verification implemented with the DRP and compact finite difference schemes for the 1-D and 2-D domain decomposition strategies, as presented earlier. It was used a mesh with 558 x 558 points in each direction and $Ma = 0.50$. In Tab. 2 are presented the E_{RMS} and can be observed that both sequential, 1-D and 2-D codes implemented with DRP-scheme as sequential, 1-D and 2-D codes implemented with compact scheme presented equal value among them, highlighting that it was not introduced any error due code paralleling procedure.

Table 2. E_{RMS} for sequential, 1-D and 2-D decomposition for both finite difference schemes.

Case	seq. compact	1-D compact	2-D compact	seq. DRP	1-D DRP	2-D DRP
E_{RMS}	$5.47 \cdot 10^{-9}$	$5.47 \cdot 10^{-9}$	$5.47 \cdot 10^{-9}$	$5.77 \cdot 10^{-9}$	$5.77 \cdot 10^{-9}$	$5.77 \cdot 10^{-9}$

5. PARALLEL COMPUTATION PERFORMANCE ANALYSIS

When paralleling a code, some parameters as *speed-up* and *efficiency* can be used to evaluate the parallel code performance. Speed-up, presented in Eq. (13), refers to how much an algorithm being processed in parallel is faster than one being processed in a single processing element. An ideal speed-up is obtained when its value is equal the number of processing elements and is called *linear*. Efficiency, presented in Eq. (14), is a typical value between 0 and 1 and estimates how much effort is spent in communication and synchronisation among the processing elements. A good efficiency presents values close to unit.

$$Sp = \frac{T_1}{T_{np}} \tag{13}$$

where np represents the number of processing elements used, T_1 and T_{np} represents the total computational time with a single processing element and with np processing elements, respectively.

$$Ef = \frac{T_1}{np \cdot T_{np}} \tag{14}$$

In the present work, it was used domain decomposition using MPI to parallel a sequential code using two different strategies, as showed in section 3. For a parallel computation performance analysis four different meshes (M1: 406x406; M2: 558x558; M3: 710x710; M4: 854x854) were used. Also were used 2, 4 and 8 processing elements to run the simulations.

From Figs. 6(a) and 6(b), which presents the speed-up behaviour for 1-D and 2-D domain decomposition strategies, respectively, it is possible verify that this parameter was higher for the cases where it was used the compact scheme than when used the DRP schemes, except for the cases when used 2 processing elements. This behaviour can be explained by the fact that it is necessary to solve an algebraic system for the compact scheme. Thus, there is an increase the number of actions performed by the code during simulation and it was optimized using the parallel procedure. Furthermore, it was observed that speed-up was higher for the 2-D domain decomposition than 1-D case. However, it was not observed linear speed-up for any case, showing that the code is losing time due to communication and synchronisation.

Figures 7(a) and 7(b) presents the efficiency results, where can be observed that, except for 2 processing elements, the efficiency is higher for the compact scheme than for DRP scheme. However, efficiency decreases at around 0.5 for 8 processing elements which corresponds to 50% of computation time spent in communication and synchronisation.

6. CONCLUSIONS

In the present work it was performed numerical study of two-dimensional waves propagation by solving LEE equations. The spatial derivatives were calculated by a 4^{th}-order DRP and a 6^{th}-order compact finite difference schemes. Additionally, the problem was parallelized adopting MPI using 1-D and 2-D domain decompositions. The verification shows that both methods gives accurate solutions, although the DRP scheme showed a small dispersion behaviour. The parallelization did not affect the results obtained. Speed-up and efficiency analysis showed that the computation time is reduced using this technique; however, there was a decrease in efficiency when the processing elements increase. This behaviour can be explained by the increase in time spent in communication and synchronization. The parallelization was more efficient when used the compact finite difference scheme.

7. REFERENCES

Colonius, T., Lele, S.K. and Moin, P., 1992. "Boundary conditions for direct computation of aerodynamic sound generation". In *14th DGLR/AIAA Aeroacoustics Conference*. pp. 438–447.

Ffowcs Williams, J.E. and Hawkings, D.L., 1969. "Sound generation by turbulence and surfaces in arbitrary motion". *Royal Society of London Philosophical Transactions Series A*, Vol. 264, pp. 321–342.

Hu, F., 1996. "On absorbing boundary conditions of linearized euler equations by a perfectly matched layer". *Journal of Computational Physics*, Vol. 129, pp. 201–219.

Hu, F., 2001. "A stable perfectly matched layer for linearized euler equations in unsplit physical variables". *Journal of Computational Physics*, Vol. 173, p. 453âĂŞ480.

Lele, S.K., 1992. "Compact finite difference schemes with spectral-like resolution". *Journal of Computational Physics*, Vol. 103, pp. 16–42.

Lighthill, M.J., 1952. "On sound generated aerodynamically. i. general theory". In *Proceedings of the Royal Society of London. Series A, Mathematical and Physical Sciences*. Vol. 211, pp. pp. 564–587.

Lighthill, M.J., 1954. "On sound generated aerodynamically. ii. turbulence as a source of sound". In *Proceedings of the Royal Society of London. Series A, Mathematical and Physical Sciences*. Vol. 222, pp. pp. 1–32.

Santana, L.D. and Souza, L.F., 2006a. "Numerical propagation of one-dimensional waves with low-dipersion and low-dissipation methods". In *Proceedings of the 5th Turbulence and Transitions Spring School - EPTT2006*. pp. ETT06–21.

Santana, L.D. and Souza, L.F., 2006b. "Numerical solution of 2-dimensional linearized euler equations for acoustic waves in flow". In *Proceedings of the 11th Brazilian Congress of Thermal Sciences and Engineering - ENCIT2006*. pp. CIT06–0432.

Tam, C.K.W., Auriault, L. and Camballi, F., 1998. "Perfectly matched layers as an absorbing boundary condition for the linearized euler equation in open and ducted domains". *Journal of Computational Physics*, Vol. 144, pp. 213–234.

Tam, C.K.W., 2006. "Recent advances in computational aeroacoustics". *Fluid Dynamics Research*, Vol. 38, No. 9, pp. 591–615.

Tam, C.K.W. and Webb, J.C., 1993. "Dispersion-relation-preserving finite difference schemes for computational acoustics". *Journal of Computational Physics*, Vol. 107, pp. 262–281.

Wang, M., Freund, J.B. and Lele, S.K., 2006. "Computational prediction of flow-generated sound". *Annual Review of Fluid Mechanics*, Vol. 38, No. 1, pp. 483–512.

Williams, J.E.F., 1963. "The noise from turbulence convected at high speed". *Philosophical Transactions of the Royal Society of London. Series A, Mathematical and Physical Sciences*, Vol. 255, No. 1061, pp. 469–503.

Y. Kalighi, A. Mani, F.H. and Moin, P., 2008. "Prediction of sound generated by complex flows at low mach number regimes". In *Center for Turbulence Research - Annual Research Briefs 2008*. pp. 313–324.

8. Responsibility notice

The authors are the only responsible for the printed material included in this paper.

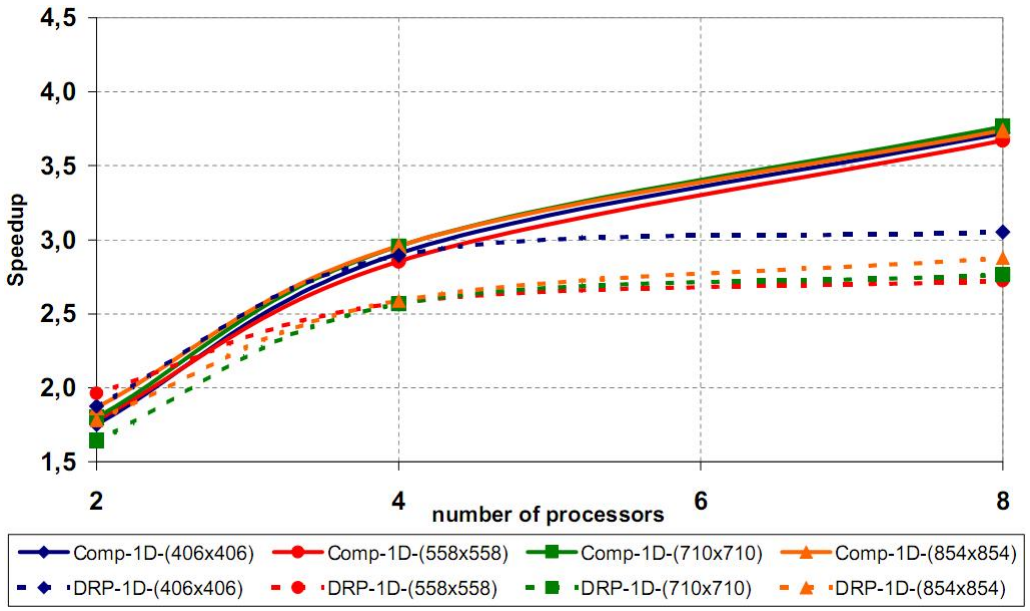

(a)

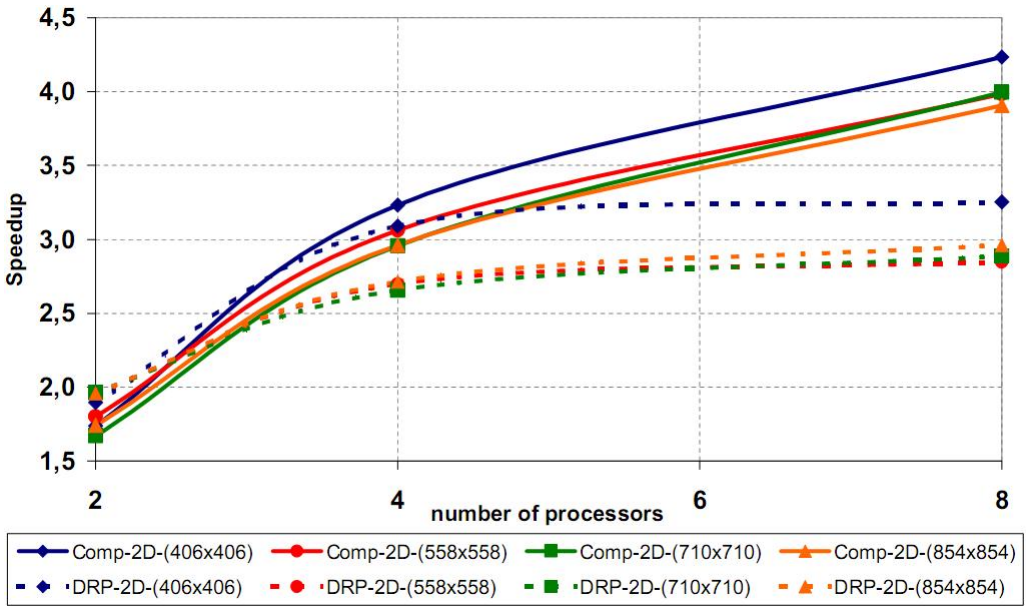

(b)

Figure 6. Speed-up for (a) 1-D domain decomposition and (b) 2-D domain decomposition

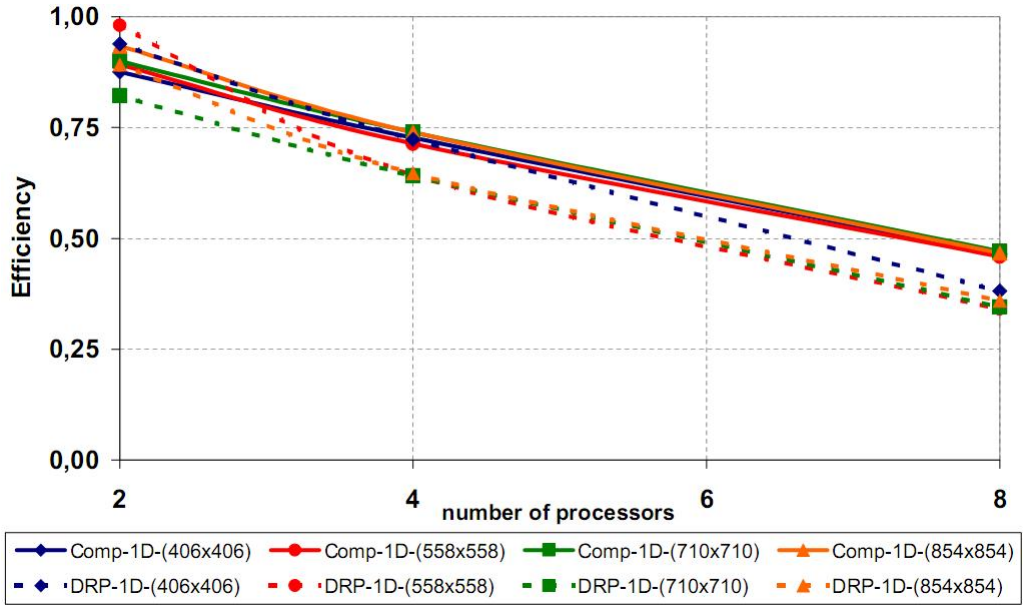

(a)

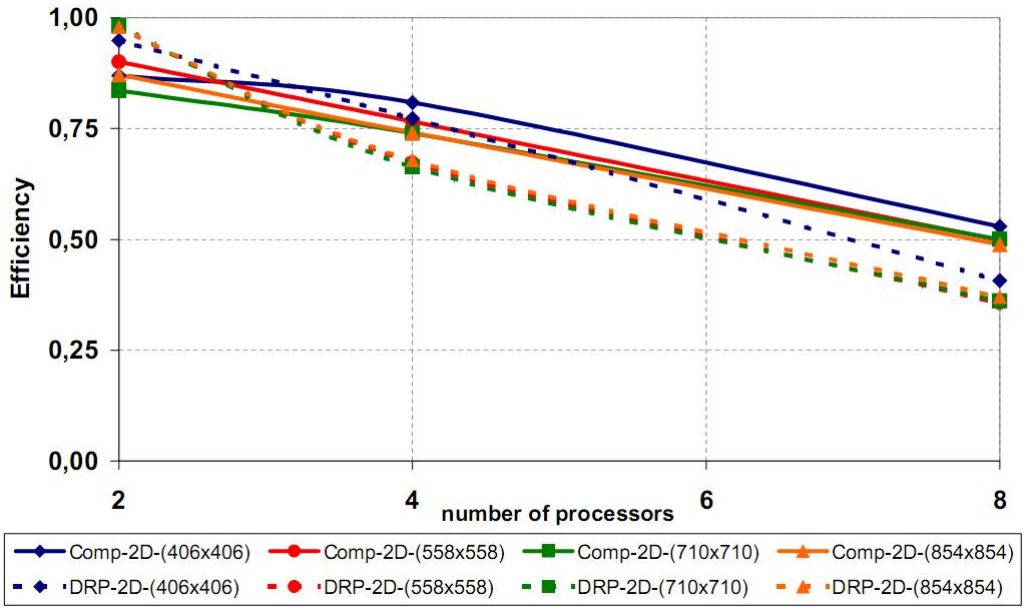

(b)

Figure 7. Efficiency for (a) 1-D domain decomposition and (b) 2-D domain decomposition